Indian Journal of Engineering & Materials Sciences
Vol. 31, June 2024, pp. 425-433
DOI: 10.56042/ijems.v31i3.7847

Adsorption of Pb(II) on modified groundnut shell (MGNS): Isotherm, kinetic, and thermodynamic study

Sheel Ratan[a], Abhishek Srivastava[b], Chinky Gangwar[a], Rashmi Nayak[c], Vartika Pandey[c], & Radhey Mohan Naik[a*]

[a]Department of Chemistry, University of Lucknow, Lucknow226007, Uttar Pradesh, India

[b]Department of Chemistry, GLA University, Mathura281006, Uttar Pradesh, India

[c]Experimental Botany and Nutraceutical Laboratory, Department of Botany,
Deen Dayal Upadhyay Gorakhpur University, Gorakhpur, Uttar Pradesh 273009, India

Received: 6 January 2024; Accepted: 19 May 2024

The environmental impact of lead compounds is significant. Lead compounds are typically consumed through drinking water and offer a substantial danger. Pb(II) and related compounds are hazardous and have been classified as probable human carcinogens by distinct regulatory authorities. For a regulatory and health standpoint, Pb(II) ion removal from wastewater and water is crucial. By sulfuric acid activation, groundnut shell (GNS) has been converted into low-cost activated carbon and grafted with EDTA to make modified groundnut shell (MGNS) powder. An analysis has been conducted on its capacity to adsorb Pb(II) ions from aquatic solutions. An MGNS sample has been examined using SEM, BET, and FTIR techniques, revealing the presence of a porous framework with a surface area of 2143 m^2/g. The absorption system adhered to a pseudo-second-order kinetic model, with the equilibrium time being determined at 120 minutes. The adsorption isotherms have been accurately simulated by the Langmuir model. A mechanism involving ion exchange has been suggested by the substantial pH dependence of Pb(II) adsorption on MGNS. Studies on regeneration have shown that MGNS can be reused repeatedly by desorbing them with HCl.

Keywords: Equilibrium time, Kinetic modeling, Langmuir adsorption isotherm, Lead, Modified groundnut shell (MGNS), pH

1 Introduction

Last few decades, researchers have more focused on the different approaches to removing heavy metals such as mercury (Hg), lead (Pb), etc. from the waste water. The existence of heavy metals in water leads to severe health issues and environmental pollution. Therefore, the presence of non-degradable, hazardous, and toxic heavy metal ions in industrial effluent has been very harmful to aquatic and human life[1,2]. The major sources of wastewater containing heavy metal ions are the industrial sector like the mining industries, metal plating, electroplating, fertilizer formation, pesticide synthesis, batteries, and textile industries[3-5]. The toxicity of heavy metals attracts more attention, and hence extra efforts of researchers are made to find out the best route for their removal. Since the toxicity related to lead(II) ions has been much higher even at very low concentrations and it possesses the highest health risk[6,7]. The toxicity of lead causes damage to the reproductive system, kidney and nervous system, brain, liver, severe stomachache, hypertension, reduced blood synthesis, and may also lead to miscarriage in pregnant women[6,7]. Lead is known to be one of the major pollutants released by metal plating, battery, ceramic & glass industries, paint & pigment manufacturing, soldering materials, finishing, explosive manufacturing, iron & steel industries, and photographic materials[8-11]. As per the Environmental Protection Agency (EPA), the acceptable concentration of lead(II) ions is 0.05mg/L in drinking water[12]. Surprisingly, the lead(II) ions concentration in industrial wastewater has been found approx. 200-500 mg/L; which is an actually very high value[13]. Therefore, it is important to find cost-effective and efficient methods to remove Pb(II) from wastewater.

In the realm of heavy metal toxicity mitigation, a plethora of techniques exist to address this concern. These techniques encompass membrane separation, ion exchange, electrolysis, adsorption, and chemical precipitation. Among the above-mentioned methodologies, adsorption has been empirically demonstrated to be a straightforward and highly efficient approach[14]. Activated carbon is extensively employed as an adsorbent in various waste water treatment applications. The material exhibits a

*Corresponding author (E-mail:naik_rm@rediffmail.com)

significantly enhanced level of porosity, showcasing a substantial internal surface area, and demonstrating commendable mechanical strength[15-17]. Despite its extensive utilization across various industries, activated carbon continues to be a material of considerable cost. Hence, it becomes imperative to conduct an in-depth exploration and advancement of cost-efficient carbon materials that can be effectively utilized for the purpose of mitigating water pollution. A diverse range of cost-effective materials has been utilized for the purpose of extracting impurities from aqueous solutions. These materials encompass algal wastes, pecan shells, palm shells, peanut hulls, coconut shells, and hazelnut husks[15-22]. Many researchers are interested in this low-cost adsorption approach because it doesn't require a sophisticated regeneration methodology.

Our research aims to evaluate the effectiveness of using modified groundnut shell (MGNS) to remove Pb(II) ions from wastewater. The investigation of GNSP properties involves the utilization of numerous analytical techniques, including FTIR, BET, and SEM. The investigation encompassed an examination of the impact of different operating parameters, including initial Pb(II) concentration, temperature, pH of the solution, adsorbent dose, and contact time. The investigation focused on studying adsorption isotherms, employing various adsorption models such as the Langmuir, Freundlich, and Temkin adsorption isotherm models. Additionally, kinetic models (pseudo-second-order and pseudo-first-order) were employed to assess the experimental data and gain insights into the adsorption behavior of Pb(II) ions onto GNPS. Thermodynamic investigations were also conducted to assess the standard free energy (ΔG^o), enthalpy change (ΔH^o), and entropy change (ΔS^o) in order to ascertain the nature of the adsorption phenomenon (endothermic or exothermic).

2 Materials and Method

2.1 Experimental

All experiment was conducted using double-deionized water (DDW) and analytical-grade reagents over the entire study. Lead nitrate (AR, Fisher Scientific, India), and EDTA (AR, Fisher Scientific, India) utilized were of utmost purity. The stock solution of 1000 mg/L of $Pb(NO_3)_2$ was prepared in double distilled water (DDW). Himedia India supplied H_2SO_4(99.9 %) which was utilized without subsequent purification. NaOH(Fisher Scientific, India), and HCl (Merck, India) solutions were employed to modulate the pH of the reacting solution using a Systronics 361 pH meter. FT-IR spectrophotometer (IR Affinity, Shimadzu) was utilized to examine the functional groups in MGNS and Pb(II)-loaded MGNS. The wave number ranges 4000-400 cm^{-1}were used to record the FT-IR spectra. Using a scanning electron microscope (S4800, Hitachi, Japan), MGNS's surface morphology and structure were observed.

2.2 Preparation of MGNS

The groundnut shell (GNS)was collected from local areas around Lucknow (India). GNS was crushed, washed thoroughly with DDW to eliminate impurities, and dried in an oven for 6-8 hours at 100 °C. After drying, the residue was ground and sieved to obtain the groundnut shell powder (GNSP) ofthe desired particle size (100 μm). GNSP (10 g) reacted with 50% sulphuric acid (100 mL) in a round bottom flask at 100 ± 2°C and kept in contact for 1hour. Afterward, the GNSP was extensively rinsed with DDW until the pH of the filtrate reached a neutral level.

Acid treatment was done to improve the sorption capacity and porosity of the adsorbent[23,24]. For grafting, 10 g of GNSP adsorbent was added to 50 ml of ethyl enediaminetetra-acetic acid (EDTA),and the mixture was continuously stirred for one hour at a temperature of 100 ± 2 °C. The MGNS underwent a drying process at a temperature of 80 °C for 12 hours. Subsequently, the MGNS was ground to acquire particles 100 μm size and later kept in a desiccator for future utilization.

2.3 MGNS adsorption experiments

Adsorption experiments using MGNS were conducted to determine the optimal conditions for the adsorption of Pb(II). For that, 0.02 g of MGNS and 50 ml of Pb(II)solution (20 mg/L)were carefully introduced into a 250 ml round bottom flask. NaOH or HCl solution was used to maintain the pH of the test solution prior to the addition of the adsorbent. At a constant temperature of 303 K, the test solutions were then shaken for 120 minutes at 150 rpm in a thermostat rotator. Subsequently, the supernatant solutions underwent filtration, and the quantification of metal content in each flask was accomplished utilizing an atomic absorption spectrophotometer (180-80, Hitachi, Japan). The uptake of Pb(II) at equilibrium, q_e (mg/g), and the % removal of Pb(II), were determined using equation 1 and 2.

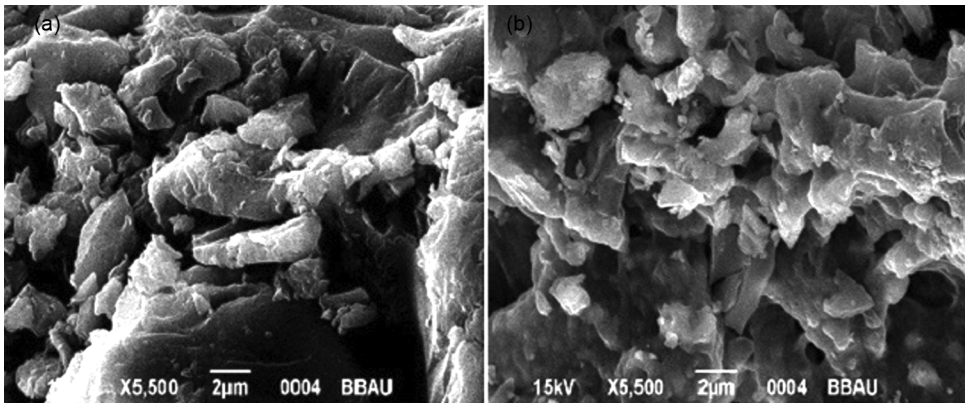

Fig. 1 — SEM images of MGNS powder at 5500 magnification (a) before adsorption of Pb(II), and (b) After adsorption of Pb(II).

$$q_e = \frac{(C_o - C_e) \times V}{m} \quad \ldots (1)$$

$$\text{Percentage Removal} = \frac{(C_o - C_e) \times V \times 100}{C_o} \quad \ldots (2)$$

Where the variables are the initial concentration of Pb(II) ions (C_o), the equilibrium concentration of Pb(II) ions (C_e), the mass of the adsorbent (m), and the volume of the solution (V).

2.4 Desorption studies

The MGNS that had been synthesized was exposed to Pb(II) (20 mg/L) until it reached a state of equilibrium. The equilibrium concentration of adsorbate, C_{ad} (mg/L), was determined by subtracting the starting concentration (C_o) from the equilibrium concentration (C_e). Subsequently, the exhausted MGNS was isolated from the solution and rinsed with DDW to eliminate any unabsorbed Pb(II) ions. After being dried at 40 ^oC in a vacuum oven, the sample was agitated for desorption experiments using DDW, 0.1 N NaOH, and HCl, in that order. Following desorption, measurements were made of the Pb(II) concentrations (mg/L) that were desorbed C_{de}. The following formula was used to get the percentage of desorption:

$$\text{Desorption} = \frac{C_{ad}}{C_{de}} \times 100 \quad \ldots (3)$$

3 Results and Discussion

3.1 Characterization of MGNS

Figure 1(a) shows the SEM image of MGNS powder prior to adsorption. The image exhibits an asymmetric, rough, and porous structure. In addition, it has micro-sized active sites or cavities, indicating that MGNS powder could be a promising adsorbent for hosting Pb(II) ions. On the other hand, Figure 1b illustrates the alterations in the morphology that were observed once Pb(II) ions were adsorbed onto the MGNS surface. The SEM image clearly shows a more compact and closely bound morphology, likely due to the binding or adsorption of Pb(II) ions onto its cavity. However, when cavities are filled with Pb(II) ions found in MGNS, the resulting surface is smoother compared to pure MGNS powder.

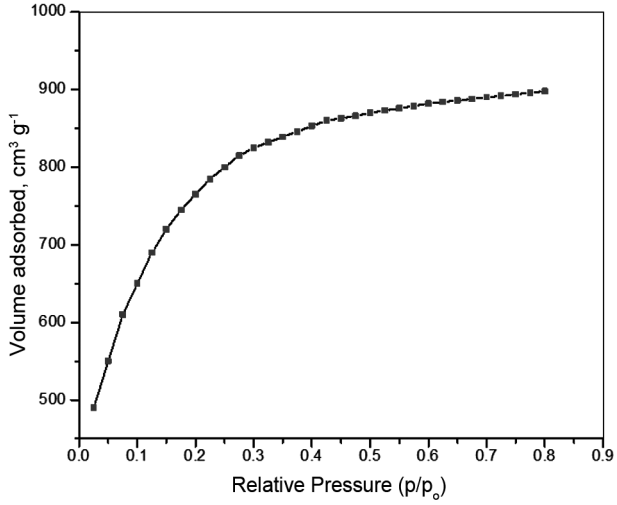

Fig. 2 — Nitrogen adsorption isotherms for prepared MGNS.

One of the most significant characteristics of adsorbents is their surface area. Figure 2 represents the nitrogen adsorption isotherms for prepared MGNS. It was discovered that MGNS had a surface area of 2143 m^2/g, which was comparatively large for the effective adsorption of metal ions. The average pore diameter of 7.8 nm suggests the mesoporous structure of MGNS[25].

In the wave number region of 4000-400 cm^{-1}, the FT-IR spectra of GNS, MGNS, and Pb(II) ions adsorbed MGNS powder have been scanned using the KBr pellet method. The FT-IR spectra of Pb(II) ions

adsorbed MGNS powder, GNS, and MGNS are shown in Fig. 3.The FTIR spectra of MGNS revealed that the absorbance bands had peaks at 3412, 2870, 1680, 1590, 1300, and 1100 cm^{-1}. Other researchers have documented the majority of these bands for various carbon compounds. A band in between 3500-3300 cm^{-1} can be ascribed to -OH and/or N-H stretching[26]. A peak between 3000-2875 cm^{-1} corresponds to alkane C-H stretching. At 1680 cm^{-1}, we observe the distinctive C=O stretching of the carboxylic acid group[27]. Peaks at 1590 and 1300 cm^{-1} are indicative of to sp^2-hybrid carbon-carbon (C=C, stretching) and sp^3-hybrid C-H bending, respectively[28]. A peak at 1100 cm^{-1} indicates C-O stretching; however, peaks below 1000 cm^{-1} are caused by distinct functional groups' bending vibrations. The presence of the –OH and NH_2 groups indicates that there has been a significant amount of interaction between the adsorbate and the adsorbent, which could help Pb(II) ions adsorb onto the MGNS's active sites.

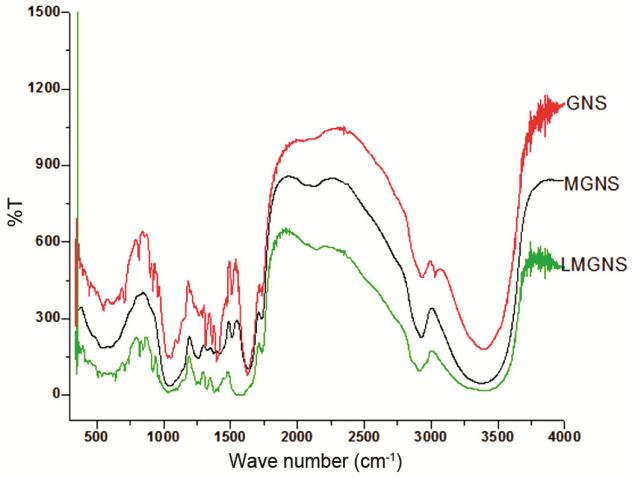

Fig. 3 — FT-IR Spectra of GNS, MGNS and LMGNS (after adsorption of Pb(II) on MGNS).

3.2 Influence of pH on Pb(II) removal

The primary variable influencing adsorption efficacy is pH because it influences the interface properties of the adsorbate and adsorbent by altering the surface charge, the behavior of the adsorbate ions in solution, and deprotonation/protonation of the functional groups on the adsorbent surface. In order to prevent Pb(II) precipitation and maximize removal efficacy, a sorption experiment was performed in the pH ranging from 1 to 6, as illustrated in Figure 4a. Pb(II) adsorption by MGNS was extremely pH sensitive; when the pH level rose from 1.0 to 5.0, the removal efficacy increased rapidly from 28.25% to 90.23%. H_3O^+ and Pb(II) competing for adsorption sites on MGNS provides an explanation for the results. There may be less adsorbed Pb(II) at low pH levels due to competition between extra H_3O^+ and Pb(II). The covered H_3O^+ leaves the MGNS surface when the pH rises, making the sites accessible to Pb(II)[29]. Furthermore, as pH rises, the amine and oxygen-containing functional groups on the surface of MGNS deprotonate, increasing the negative charge on the MGNS surface[30]. As a result, Pb(II) adsorption increased due to the increased electrostatic attraction between MNGS and Pb(II). Surprisingly, with further change in pH values from 5.0 to 6.0, no considerable changes have been observed in % removal of Pb(II) ions. Therefore, the subsequent experiments have been performed at pH 5.

3.3 Influence of MGNS dose on Pb(II) removal

The amount of adsorbent utilized is one of the most crucial variables that affects how well the adsorption

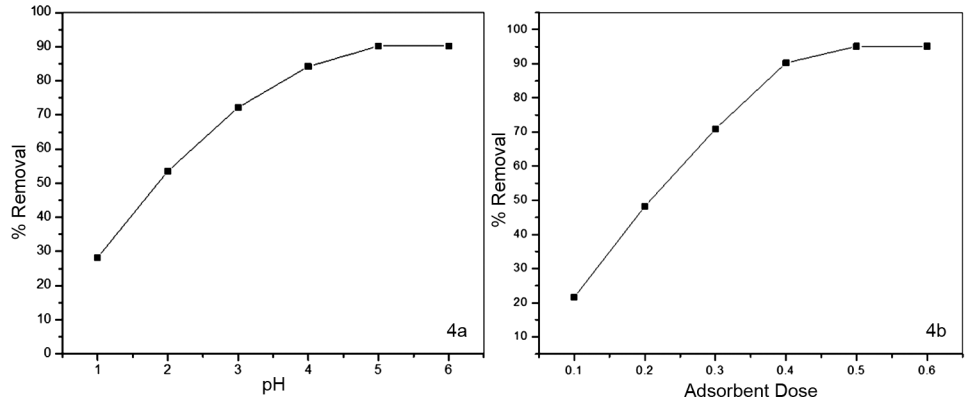

Fig. 4 — (a) Influence of pH on % removal of Pb(II) at [Pb(II)] = 20 mg/L, MGNS dose = 2.0 g/L, Temperature = 303 K, and Contact time = 120 min, & (b) Influence of MGNS dose on % removal of Pb(II) at [Pb(II)] = 20 mg/L, pH = 5.0 ± 0.1, Temperature = 303 K, and Contact time = 120 min.

process goes. Removal effectiveness usually increases with an increase in the adsorbent dosage. At considerably greater adsorbent dosages, however, there was no discernible difference in removal efficiency. To determine the optimum value of adsorbent for Pb(II) removal, the MGNS dose was varied from 0.1 to 0.6 g/L. Figure 4(b) illustrates that when the MGNS dose is increased from 0.1 to 0.6 g/L, the elimination of Pb(II) ions increases from 21.59 to 95.11%. At higher doses, the adsorbent's large surface area and more active adsorbing sites (more availability of functional groups) are responsible for the constant increase in adsorption effectiveness. Higher doses of the adsorbent, however, cause the active adsorbing sites to agglomerate and overlap, reducing surface area and active adsorbing sites and maintaining a constant adsorption capacity[31,32].

3.4 Study of variation contact time

Adsorption, a time-dependent phenomenon, plays a pivotal role in the conceptualization of novel adsorption systems. The temporal interplay between metal ions and adsorbents facilitates the elucidation of the kinetic propensity for binding and sequestration of metal ions, alongside the identification of the optimal time range for achieving maximal removal efficiency. The observed trend in the % removal of Pb(II) ions as a function of contact time is depicted in Fig. 5(a). Initially, it has been observed that the rate of adsorption exhibits a rapid increase during the initial 60 minutes. Subsequently, the rate experiences a gradual increase until reaching 120 minutes, at which point it stabilizes, indicating the attainment of adsorption equilibrium. The initial swift adsorption can be attributed to the robust affinity between the Pb(II) ions and the active sites of the adsorbent[33,34]. As the procedure advanced, the rate of adsorption reduced decreased because the active sites of MGNS were gradually being occupied. The saturation of the MGNS's active sites is what causes the consistency in the adsorption rate.

3.5 Study of variation of lead(II) ions solution concentration

The starting metal ion concentration plays a crucial role in establishing the adsorption rate for effective adsorption. With an increase in Pb(II) concentration from 10 ml/L to 50 mg/L, the percentage removal of Pb(II) decreases from 96.45% to 22.55% Fig. 5(b). This is because the MGNS dosage was constant, which limited the total number of accessible active sites of MGNS and decreased the efficacy of Pb(II) removal.

3.6 Adsorption Isotherms

To explore the adsorption and the mechanisms involved during the process, adsorption isotherm models such as Langmuir, Freundlich, and Temkin were used to fit the Pb(II) adsorption data on MGNS.

At equilibrium, the Langmuir adsorption equation for a monolayer of adsorbate adsorbed onto the adsorbent surface with finite active sites can be expressed as[35]:

$$\frac{C_e}{q_e} = \frac{1}{q_{max}K_L} + \frac{C_e}{q_{max}} \quad \ldots (4)$$

Where, q_e(mg/g) denotes the quantity of Pb(II) ions adsorbed on MGNS at equilibrium; the equilibrium concentration of the Pb(II) ions in solution is C_e (mg/L); the monolayer adsorbate adsorption

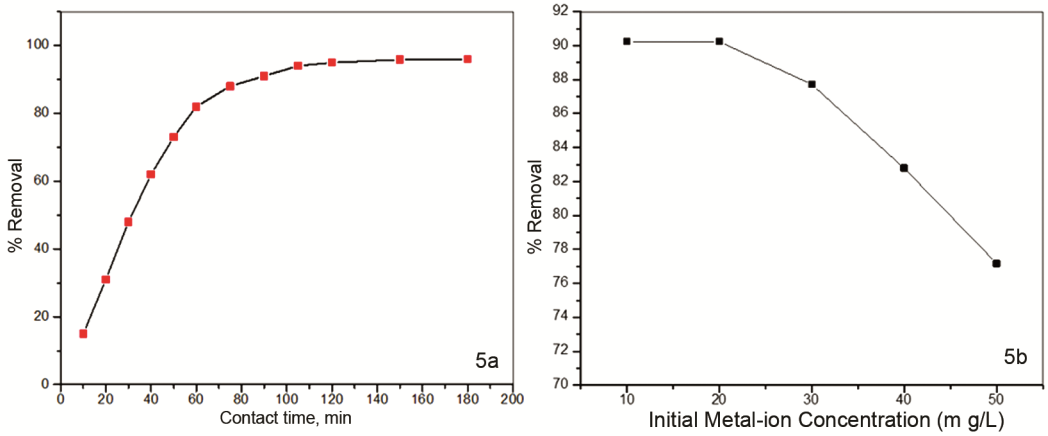

Fig. 5 — (a) Influence of contact time on % removal of Pb(II) at MGNS dose = 2.0 g/L, pH = 5.0 ± 0.1, Temperature = 303 K, and [Pb(II)] = 20 mg/L, & (b) Influence of [Pb(II)] on % removal of Pb(II) at MGNS dose = 2.0 g/L, pH = 5.0 ± 0.1, Temperature = 303 K, and Contact time = 120 min.

performance or capacity isq_{max}(mg/g); and Langmuir constant is K_L (L/mg). Langmuir constant is associated with the free energy of adsorption. Figure 6a depicts a plot of C_e/q_e vs C_e, exhibiting a linear relationship. The values of q_{max} and K_L can be determined by examining the slope (1/ q_{max}) and intercept (1/ q_{max} K_L) of the plot. These values are recorded in Table 1. The linearity observed in the plot depicted in Fig. 6(a) serves as evidence supporting the validity of the LMA model. The outcomes of our investigation's calculation of the monolayer adsorption performance or capacity are superior to those of the previously published work[36-40]. Table 2 provides a comparison of the current work's monolayer adsorption capacity values with those found in the literature.

The following equation is used to define a dimensionless equilibrium parameter R_L, which is used to assess the adsorption's favorability:

$$R_L = \frac{1}{1 + K_L C_o} \quad \ldots (5)$$

where, the initial concentration of lead(II) is C_o (mg/L); and Langmuir constant is K_L (L/mg). The isotherm type can be classified as irreversible (R_L = 0), linear (R_L = 1), unfavorable (R_L> 1), or favorable (0< R_L< 1) based on the RL value[41].

Table 1 — Langmuir, Freundlich, and Temkin isotherm constants for the Pb(II) adsorption onto MGNS

Isotherm	Constant Values
Langmuir	q_{max}(mg/g) = 133.33
	K_L(L/mg) = 0.24
	R^2 = 0.99
	R_L= 0.29-0.077
Freundlich	K_F(mg/g) = 26.90
	n = 1.74
	R^2 = 0.94
Temkin	B = 25.54
	b (J/mol) = 30.089
	R^2 = 0.99
	A (L/g)= 6.5385

The Freundlich model is suited to highly heterogeneous surfaces and multi-layer adsorption with no plateau. Equation 6 provides the formula for the Freundlich adsorption isotherm[42].

$$log q_e = log K_F + \frac{1}{n} log C_e \quad \ldots (6)$$

Where, q_e(mg/g) denotes the quantity of Pb(II) ions adsorbed on MGNS at equilibrium; the equilibrium concentration of the Pb(II) ions in solution is C_e (mg/L); and K_L and n Freundlich constants. Figure 6(b) depicts that the plot of ln q_e vs ln C_e is linear in nature. Table 1 shows the values of n and K_F, which were determined from the slope (1/n) and the intercept (ln K_F) of the plot. The value of n indicates the adsorption's favorability. There is a typical Langmuir isotherm if the value of 1/n is smaller than 1.

The expression used for Temkin isotherm is given in equation 7[43]:

$$q_e = B\, lnA + B\, lnC_e \quad \ldots (7)$$

Where the equilibrium binding constant, A, belongs to the highest binding energy, while the Temkin constant, B J/mol, is associated with the heat of adsorption. Figure 6(c) shows the Temkin model isotherm (q_e vs ln C_e plot). The slope and intercept of the isotherm were utilized to calculate B and A. All the calculated values from Temkin isotherm have been listed in Table 1.

The Pb(II) adsorption onto MGNS exhibited excellent conformity to the Langmuir isotherm model,

Table 2 — Comparative studies of the lead(II) adsorption capacities onto various adsorbents

Adsorbent	q_{max} (mg g^{-1})	Reference
Coconut activated charcoal	53.7	31
Date palm trunk	53.8	13
Leaf of date trees	55.56	30
Coffee residue	89.28	33
Cactus cladodes	98.62	32
MGNS	133.33	Present Study

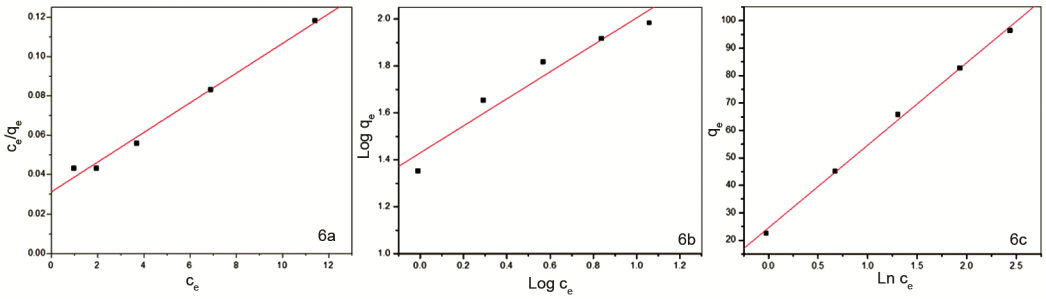

Fig. 6 — Plot of (a) Langmuir, (b) Freundlich, and (c) Temkin, isotherm model for the adsorption of Pb(II) on MGNS.

as evidenced by the high R^2 value of 0.99. This outcome can be attributed to the uniform dispersion of active sites across the MGNS surface. Moreover, the observed R_L values for the Langmuir isotherm fell within the range of 0 to 1, while the Freundlich constant 1/n exhibited a value less than 1, thereby suggesting a process that is thermodynamically favorable. Table 2 presents a comparative analysis of the adsorption capacity for Pb(II) in relation to various activated carbons derived from solid waste materials. The significant adsorption capacity exhibited by this paper elucidates the potential utilization of MGNS as a highly promising adsorbent for the efficient removal of Pb(II).

3.7 Adsorption Kinetics

The kinetic investigation for Pb(II) adsorption onto MGNS has been done utilizingLagergren'sfirst-order model, and Ho-McKay's second-order kinetic model.

First-order model, whichis often provided by Equation 8, is dependent on the solid adsorbent capacity[44].

$$log(q_e - q_t) = logq_e - \frac{k_1}{2.303}\, t \qquad \ldots (8)$$

Where, q_e(mg/g) denotes the quantity of Pb(II) ions adsorbed on MGNS at equilibrium, andq_t (mg/g) respectively and the adsorption rate constant is k_1 (min^{-1}).Figure 7(a) displays a plot of log ($q_e - q_t$) vs time (t), which has been used to compute the values of the adsorption rate constant (k_1). Table 3 provides a summary of every parameter that was computed with this model. Based on the lower values of the regression coefficient (adj. R^2), it appears that this model is not providing the best fit and may not be suitable for the current conditions.

Based on equilibrium adsorption, the pseudo-second-order (PSO) model has been presented as[45]:

$$\frac{t}{q_t} = \frac{1}{k_2 q_e^2} + \frac{t}{q_e} \qquad \ldots (9)$$

where, k_2 (g/mg min), qe (mg/g), and qt (mg/g) are the pseudo-second-order rate constant, amount of Pb(II) adsorbed on MGNS at equilibrium and at different times respectively. Figure 7(b) illustrates the linear relationship between t/q_t and time t. The values of q_e and k_2 can be found on this graph by using the slope and intercept, respectively. Table 3 has the calculated values listed.

Upon comparing the outcomes of the regression coefficients, it is observed that R^2 exhibited a value of 0.999 when considering the second-order reaction kinetics. Conversely, when considering the first-order reaction kinetics, R^2 displayed a value of 0.961. These findings indicate that the adsorption kinetics of Pb(II) on MGNS adhere to the principles of second-order kinetics.

Table 3 — Parameters calculated from PFO and PSO kinetic model

Kinetic Model	Constant Values
Pseudo first order	$q_{e(exp)}$(mg/g) = 47.56
	$q_{e\,(cal)}$(mg/g) = 32.55
	$k_1(min^{-1})$ = 0.021
	R^2 = 0.961
Pseudo second order	$q_{e(exp)}$(mg/g) = 52.91
	k_2(g mg^{-1} min^{-1}) = 0.001
	R^2 = 0.999

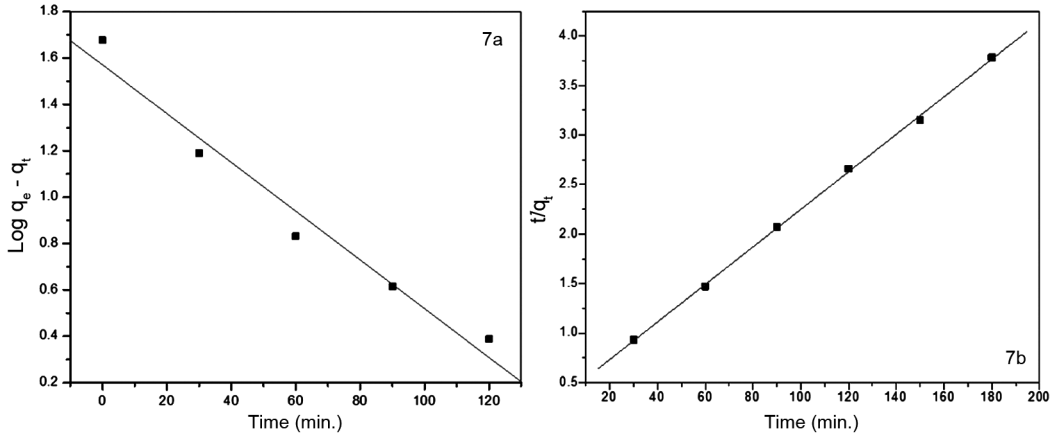

Fig. 7 — (a) Pseudo-first order (PFO) and (b) Pseudo-second order, plot for adsorption of Pb(II) on MGNS.

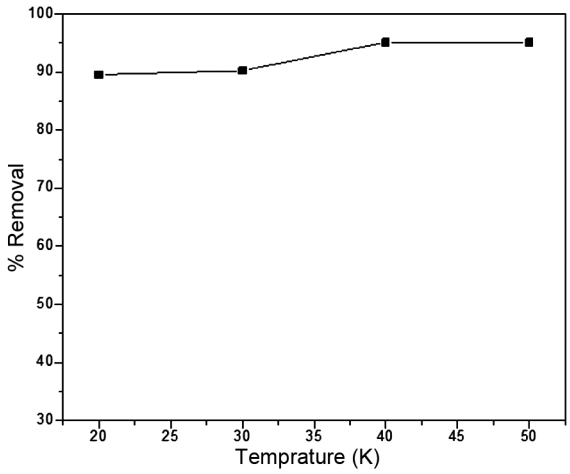

Fig. 8 — Influence of temperature on % removal of Pb(II) at MGNS dose = 2.0 g/L, pH = 5.0 ± 0.1, [Pb(II)] = 20 mg/L, and Contact time = 120 min

Table 4 — Thermodynamic parameters for the adsorption of lead(II) from solution onto MGNS

T (K)	K_c	ΔG□ (kj/mol)	ΔH0	ΔS0	R^2
293	3.3495	-1.186	44.11	160.65	0.99
303	6.6306	-3.800			
313	9.2401	-6.430			
323	19.4813	-18.685			

3.8 Thermodynamic studies

The investigation of how temperature affects experimental conditions has also been crucial. The temperature effect on the % removal of Pb(II) ion is depicted in Fig. 8. With the increase in temperature, the adsorption of Pb(II) ions onto MGNS significantly increases, possibly as a result of higher kinetic energy.

Equation 10-12 was used to evaluate the thermodynamic activation parameters. Equation 10 provides the relationship between the equilibrium constant K_c and standard Gibbs free energy (ΔG°) at any temperature T.

$$\Delta G^\circ = -RT \ln K_C \quad \ldots (10)$$

Equation 11 provides the relationship between the entropy (ΔS°) and enthalpy (ΔH°) of adsorption with the standard free energy change (ΔG°), while equation 12 defines K_c.

$$lnK_c = -\left(\frac{\Delta G^o}{RT}\right) = -\left(\frac{\Delta H^o}{RT}\right) + \left(\frac{\Delta S^o}{R}\right) \quad \ldots (11)$$

$$K_C = \frac{C_a}{C_e} \quad \ldots (12)$$

Where the equilibrium concentration is C_e, and the quantity of Pb(II) ions adsorbed at equilibrium is C_a. The calculated values of the various parameters have been summarized in Table 4. The adsorption of Pb(II) ions onto MGNS appears to be endothermic, as indicated by the positive value of ΔH°. It is possible that the higher ΔS° is a result of the interaction between the solid and solution at the interface, where the Pb(II) ions are adsorbed onto MGNS. Furthermore, the negative ΔG° suggests that the adsorption of Pb(II) ions onto MGNS occurs spontaneously.

3.9 Desorption and Reusability of MGNS

Desorption investigations aid in clarifying the adsorption process and the viability of recovering the used activated carbon. The research revealed that weak interactions like Van der Waals forces can be used to explain how an ion is attached to an adsorbent if the ions that are absorbed on the solid surface can be desorbed by water[46]. If the ion is desorbable by acidic or alkaline water, an ion exchange takes place during the adsorption process. The desorption percentages of H_2O, 0.1 M MaOH, and 0.1 M HCl were determined to be 0.24%, 3.64%, and 78.23% respectively. This outcome was anticipated since the presence of acidic conditions allowed H_3O^+ ions to protonate the adsorbent surface, hence facilitating the desorption of positively charged Pb(II). Moreover, a mechanism involving ion exchange was identified, and it was found that HCl is an effective reagent for regenerating the Pb(II)-loaded MGNS. Afterward, the impact of five successive adsorption-desorption runs on the Pb(II) adsorption by MGNS was investigated. The desorbed MGNS proved to be extremely efficient in readsorbingPb(II), with the recycled Pb(II)-MGNS showing a slight decrease in adsorption capacity of approximately 5.9% by the fifth cycle. It may be inferred that the Pb(II)-MGNS can be employed multiple times without drastically reducing its adsorption capabilities.

4 Conclusion

Current research examines Pb(II) ion adsorption on modified groundnut shells (MGNS) in aqueous medium. For optimal adsorption of Pb(II) ions onto MGNS, a pH value of 5 was determined to be the most effective, with an adsorption capacity of 133.33 mg/g. It also shows that the absorption of Pb(II) ions was fast until 60 minutes, after which it reached equilibrium at 120 minutes. The substantial pH

dependence of Pb(II) adsorption on MGNS suggests a mechanism involving ion exchange. The adsorption proceeds according to pseudo-second-order kinetics, and the Langmuir isotherms provide a good fit for the equilibrium data. MGNS exhibits a remarkable capacity for regeneration. Thus, PLAC shows promise as a cost-effective and efficient adsorbent for adsorbing Pb(II) ions from water-based solutions.

References

1 Das S, Sultana K W, Ndhlala A R, Mondal M, & Chandra I, *Environ Health Insights*, 17 (2023) 11786302231201259.
2 Mitra S, Chakraborty A J, Tareq A M, Emran T B, Nainu F, Khusro A, Idris A M, Khandaker M U, Osman H, Alhumaydhi F A, &Simal-Gandara J, *J King Saud Univ Sci*, 34 (2022) 101865.
3 Odumbe E, Murunga S, & Ndiiri J, *Heavy Metals in Wastewater Effluent: Causes, Effects, and Removal Technologies* (IntechOpen, London, UK), 2023. https://doi.org/10.5772/intechopen.1001452
4 Hama Aziz K H, Mustafa F S, Omer K M, Hama S, Hamarawf R F, & Rahman K O, *RSC Adv*, 13 (2023) 17595.
5 Kapoor D, &Singh M P, *10 - Heavy metal contamination in water and its possible sources* (ElsevierScience Publishers, New York), 2021, 179.
6 Wani A L, Ara A, & Usmani J A, *Interdiscip Toxicol*, 8 (2015) 55.
7 Assi M A, Hezmee M N, Haron AW, Sabri M Y, & Rajion M A, *Vet World*, 9 (2016) 660.
8 Moore R Z, Wilson V, Hou A, &Meng G, *Int J Health Animal Sci Food Saf*, 2 (2015) 18.
9 Hama Aziz K H, Mustafa F S, Omer K M, Hama S, Hamarawf R F, & Rahman K O, *RSC Adv*, 13 (2023) 17595.
10 Cheng H, &Hu Y, *Environ Pollut*, 158 (2010) 1134.
11 Bhuiyan M A H, Parvez L, Islam M A, Dampare S B, & Suzuki S, *J Hazard Mater*,173 (2010) 384.
12 Yadav S K, Singh D K, &Sinha S, *Desalin Water Treat*, 51 (2013) 6798.
13 Liang S, Guo X, &Tian Q, *Desalin Water Treat*, 51 (2013) 7166.
14 Goswami M K, Srivastava A, Dohare R K, Tiwari A K, & Srivastava A, *Environ SciPollut Res*, 30 (2023) 73031.
15 Muttil N, Jagadeesan S, Chanda A, Duke M, &Singh S K, *Appl Sci, 13 (2023)* 257.
16 Wang B, Lan J, Bo C, Gong B, & Ou J, *RSC Adv*, 13 (2023) 4275.
17 Ani J U, Akpomie K G, &Okoro U C, *Appl Water Sci*, 10 (2020) 69.
18 Futalan C C, Diana E, Edang M F A, Padilla J M, Cenia M C, &Alfeche D M, *Sustainability*, 15 (2023) 15955.
19 Alsohaimi I H, Alhumaimess M S, Hassan H M A, Reda M, Aldawsari A M, Chen Q, &Kariri M A. *Polymers*, 15 (2023) 2188.
20 Namasivayam C, &Kavitha D, *Microchem J*, 82 (2006) 43.
21 Schneider R M, Cavalin C F, Barros M, &Tavares C R G, *Chem Eng J*, 132 (2007) 355.
22 Ali S W, Waqar F, Malik M A, Yasin T, &Muhammad B, *J App Polym Sci*, 129 (2013) 2234.
23 Kumar A, &Jena H M, *Results Phys*, 6 (2016) 651.
24 Díaz-Díez M A, Gómez-Serrano V, & Fernández González C, *Appl Surf Sci*, 238 (2004) 309.
25 Ryu Z, Zheng J, Wang M, &Zhang B, *Carbon*, 37 (1999) 1257.
26 Aguilar C, Garcıía R, Soto-Garrido G, &Arriagada R, *Appl Catal B–Environ*, 46 (2003) 229.
27 Moreno-Castilla, C, Lopez-Ramon, M.V, &Carrasco-Marın, F, *Carbon*, 38 (2000) 1995.
28 Abdel-Nasser A, &El-Hendawy A A, *Carbon*, 41 (2003) 713.
29 Rengaraj S, Joo C K, Kim Y, &Yi J, *J Hazard Mater*, 102 (2003) 257.
30 Wang L, Zhang J, Zhao R, Li Y, Li C, & Zhang C, *Bioresour Technol*, 101 (2010) 5808.
31 Tee G T, Gok X Y, & Yong W F, *Environ Res*, 212 (2022) 113248.
32 Xiaosan S, Boyang S, Yiru W, Jie Z, Sanfan W, & Nan W, *RSC Adv*, 12 (2022) 19917.
33 Xia Y, Li Y, & Xu, *Toxics*, 10 (2022) 291.
34 Gu S, Wang L, Mao X, Yang L, & Wang C, *Materials*, 11 (2018) 514.
35 Langmuir I, *J Am Chem Soc*, 40 (1918) 1361.
36 Iqbal M, Saeed A, & Zafar S I, *J Hazard Mater*, 164 (2009) 161.
37 Boudrahem F, Aissani-Benissad F, & Soualah A, *J Chem Eng Data*, 56 (2011) 1804.
38 Barka N, Abdennouri M, El Makhfouk M, & Qourzal S, *J Environ Chem Eng*, 1 (2013) 144.
39 Huang K, & Zhu H, *Environ Sci Pollut Res*, 20 (2013) 4424.
40 Yadav S K, Singh D K, & Sinha S, *Desalin Water Treat*, 51 (2013) 6798.
41 Weber T W, & Chakkravorti R K, *Am Inst Chem Eng J*, 20 (1974) 228.
42 Freundlich H, *Phys Chem Soc*, 40 (1906) 1361.
43 Temkin M I, &Pyzhev V, *Acta Physiochim URSS*, 12 (1940) 327.
44 Kalavathy M H, Karthikeyan T, & Rajgopal S, *J Colloid Interf Sci*, 292 (2005) 354.
45 Li Y H, Di Z C, Ding J, Wu D H, Luan Z K, & Zhu Y Q, *Water Res*, 39 (2005) 605.
46 Namasivayam C, &Yamuna R T, *Water Air Soil Pollut*, 65 (1992) 101